Infrared Spectroscopy of Arginine Cation Complexes: Direct Observation of Gas-Phase Zwitterions

ARTICLE *in* THE JOURNAL OF PHYSICAL CHEMISTRY A · DECEMBER 2007

Impact Factor: 2.69 · DOI: 10.1021/jp074859f · Source: PubMed

7 AUTHORS, INCLUDING:

Nicolas Polfer
University of Florida
81 PUBLICATIONS **2,956** CITATIONS
SEE PROFILE

Robert C. Dunbar
Case Western Reserve University
245 PUBLICATIONS **6,468** CITATIONS
SEE PROFILE

Infrared Spectroscopy of Arginine Cation Complexes: Direct Observation of Gas-Phase Zwitterions

Matthew W. Forbes,[†] Matthew F. Bush,[‡] Nick C. Polfer,[§,⊥] Jos Oomens,[§] Robert C. Dunbar,[||] Evan R. Williams,[‡] and Rebecca A. Jockusch*[,†]

Department of Chemistry, University of Toronto, Toronto, Ontario M5S 3H6, Canada, Department of Chemistry, University of California at Berkeley, Berkeley, California 94720-1460, FOM Institute for Plasma Physics "Rijnhuizen", Edisonbaan 14, 3439 MN Nieuwegein, The Netherlands, and Chemistry Department, Case Western Reserve University, Cleveland, Ohio 44106

Received: June 21, 2007; In Final Form: August 14, 2007

The structures of cationized arginine complexes $[Arg + M]^+$, (M = H, Li, Na, K, Rb, Cs, and Ag) and protonated arginine methyl ester $[ArgOMe + H]^+$ have been investigated in the gas phase using calculations and infrared multiple-photon dissociation spectroscopy between 800 and 1900 cm^{-1} in a Fourier transform ion cyclotron resonance mass spectrometer. The structure of arginine in these complexes depends on the identity of the cation, adopting either a zwitterionic form (in salt-bridge complexes) or a non-zwitterionic form (in charge-solvated complexes). A diagnostic band above 1700 cm^{-1}, assigned to the carbonyl stretch, is observed for $[ArgOMe + H]^+$ and $[Arg + M]^+$, (M = H, Li, and Ag), clearly indicating that Arg in these complexes is non-zwitterionic. In contrast, for the larger alkali-metal cations (K^+, Rb^+, and Cs^+) the measured IR-action spectra indicate that arginine is a zwitterion in these complexes. The measured spectrum for $[Arg + Na]^+$ indicates that it exists predominantly as a salt bridge with zwitterionic Arg; however, a small contribution from a second conformer (most likely a charge-solvated conformer) is also observed. While the silver cation lies between Li^+ and Na^+ in metal-ligand bond distance, it binds as strongly or even more strongly to oxygen-containing and nitrogen-containing ligands than the smaller Li^+. The measured IR-action spectrum of $[Arg + Ag]^+$ clearly indicates only the existence of non-zwitterionic Arg, demonstrating the importance of binding energy in conformational selection. The conformational landscapes of the Arg−cation species have been extensively investigated using a combination of conformational searching and electronic structure theory calculations [MP2/6-311++G(2d,2p)//B3LYP/6-31+G(d,p)]. Computed conformations indicate that Ag^+ is di-coordinated to Arg, with the Ag^+ chelated by both the N-terminal nitrogen and N^{η} of the side chain but lacks the strong M^+−carbonyl oxygen interaction that is present in the tri-coordinate Li^+ and Na^+ charge-solvation complexes. Experiment and theory show good agreement; for each ion species investigated, the global-minimum conformer provides a very good match to the measured IR-action spectrum.

Introduction

Amino acids exist as zwitterions in solution over a wide range of pH. Within proteins and peptides, charge localization often contributes stabilizing interactions that aid in the formation of secondary and higher-order structure and is also important for many biological functions including catalysis and ion transport.[1] The drive to better understand the balance of forces controlling structural selection has resulted in significant attention paid to the question of whether amino acids, peptides, and proteins retain their zwitterionic forms in the gas phase or isomerize to their canonical (non-zwitterionic) form in the absence of solvent.

All ground-state neutral amino acids exist in their canonical form when isolated. For example, the zwitterionic form of glycine (Gly), the simplest amino acid, is ∼90 kJ mol^{-1} higher in energy than the non-zwitterion, with no barrier for proton transfer.[2] Zwitterionic forms of amino acids can be preferentially stabilized by increased proton affinity. Thus, for arginine (Arg), which has a relatively high proton affinity due to its guanidino side chain (1051 kJ mol^{-1} compared to that of Gly, 856 kJ mol^{-1}),[3] the zwitterionic form is within 15 kJ mol^{-1} of the non-zwitterion.[4] The proton affinity of standard amino acids can be further increased by derivatization (e.g., methylation of the side chain or N-terminal amino group); this has been shown to preferentially stabilize the zwitterionic forms of selected amino acids.[5−10] Zwitterionic forms of amino acids can also be preferentially stabilized by noncovalent interactions with polar molecules such as water[2,9,11−16] or with ions (resulting in species with a net charge in the latter case).[4,8,17−21] Mass spectrometric investigations have played a leading role in characterization of such charged gas-phase amino acid conformations utilizing several methodologies including ion mobility chromatography,[22−24] collision-induced dissociation (CID),[18,25−30] blackbody infrared radiative dissociation (BIRD),[9,11,12,15,31] infrared multiple-photon dissociation (IRMPD),[10,32−55] and hydrogen/deuterium (H/D) exchange.[25,56−58]

Jockusch et al.[18] investigated the structures of Arg−alkali-metal ion complexes using both theory and electrospray

* Author to whom correspondence should be addressed. E-mail: rebecca.jockusch@utoronto.ca.
[†] University of Toronto.
[‡] University of California, Berkeley.
[§] FOM Institute for Plasma Physics "Rijnhuizen".
[||] Case Western Reserve University.
[⊥] Present address: Department of Chemistry, University of Florida, Gainesville, Florida 32611.

10.1021/jp074859f CCC: $37.00
Published on Web 11/01/2007

SCHEME 1: Representation of the Charge-Solvated and Salt-Bridge Conformers of Sodiated Arg

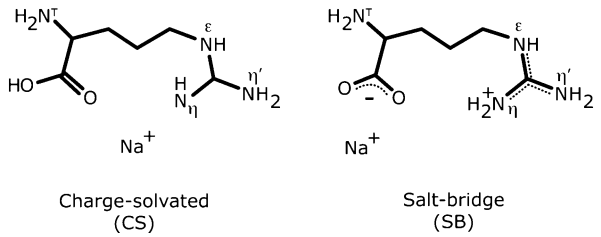

ionization mass spectrometry (ESI-MS)-based experiments to determine the effect of metal ion identity on the form of Arg present. Arg−metal ion complexes can be classified into two general categories shown in Scheme 1. When Arg is in its canonical form (having neutral guanidino side chain and C-terminal carboxylic acid groups), the resulting complex is referred to as being charge-solvated (CS). Alternatively, the zwitterionic form of Arg (having the guanidino side chain protonated and the C-terminal carboxylic acid group deprotonated) can be stabilized by the formation of a salt bridge (SB) in which the cation interacts with the deprotonated C-terminal group. CID and BIRD data, supported by density functional theory (DFT) calculations, suggested that arginine favors charge-solvated conformations with smaller cations (H^+ and Li^+) but that for the larger metals (K^+, Rb^+, and Cs^+) the salt-bridge conformer is increasingly stabilized.[18] Specifically, $[Arg + H]^+$, $[Arg + Li]^+$, and $[Arg+Na]^+$ dissociate by loss of H_2O (suggesting a C-terminus that is not deprotonated, hence a CS conformation) while $[Arg + K]^+$, $[Arg + Rb]^+$, and $[Arg+Cs]^+$ dissociate by loss of NH_3 (suggesting a C-terminal carboxylic acid group that is deprotonated, yielding a SB conformation). Although sodiated arginine fragmented by losing H_2O (suggesting a CS conformer), DFT calculations identified the global minimum to be a SB conformer. While clearly illustrating the size dependence of the alkali-metal cation on zwitterion stability, the dissociation experiments are sensitive to differences in energies between populated low-energy states and transition states for product ion formation. A small difference in dissociation energies between two competing pathways for fragmentation, as appears to be the case for the loss of water versus ammonia from these ions, can influence the relative abundances of product ions observed.[18,51]

An alternative approach to investigate conformations of gaseous molecules, complexes, and clusters is infrared spectroscopy. For example, cavity ring-down laser absorption spectroscopy has verified that isolated neutral arginine exists in its canonical conformation.[59] Unfortunately, absorption measurements such as these have inherently low sensitivity, and it is difficult to achieve sufficient sample concentrations in the gas phase to compensate. Recently, IR photodissociation using a tunable light source has been used successfully to produce IR "action" spectra of biologically relevant ions.[10,33,35−51,54,55] Briefly, gaseous ions are mass-selected and subject to IR irradiation, which is scanned over the spectral region of interest. Resonant absorption of (multiple) photon(s) increases an ion's internal energy, and dissociation can occur. By monitoring the precursor and product ion intensities as a function of excitation wavelength, a signature IR-action spectrum is measured. When supported by electronic structure theory calculations, the measured action spectra can be compared with calculated IR absorption spectra to aid conformational assignment.

IR-action spectroscopy of mass-selected ions has been performed using table-top IR lasers, which are often limited to the hydride stretching region (2500−3800 cm^{-1}),[48−51] and free electron lasers (FELs),[60,61] which provide access down to 200 cm^{-1}. Several studies have reported investigations of amino acid−metal complexes.[10,33,42,43,47,51] Kapota et al.[33] were the first to apply these methods to study the conformations of sodiated glycine and proline (Pro) isolated in a Fourier transform ion cyclotron resonance (FT-ICR) mass spectrometer. Characteristic bands assigned to the carbonyl stretch (1727 cm^{-1}) of sodiated Gly and the antisymmetric carboxylate stretches (1698 cm^{-1}) of sodiated Pro served to distinguish the charge-solvated conformers from the salt-bridge conformers. Schäfer et al.[47] reported IRMPD-action spectra of sodiated and potassiated Arg. However, structural assignment was hampered by the low resolution of the recorded spectra. Polfer et al. measured gas-phase IR spectra of $[tryptophan + M]^+$ complexes (M = Li, Na, K, Rb, Cs, and Ag)[42] and $[phenylalanine + Ag]^+$,[43] ruling out the presence of salt-bridge conformers for the monovalent metal complexes.

Very recently, Bush et al.[51] reported IR photodissociation spectra of cationized Arg species in the 2600−3800 cm^{-1} region acquired using a Nd:YAG pumped optical parametric oscillator/optical parametric amplifier (OPO/OPA) tunable laser coupled to an FT-ICR mass spectrometer. Structural assignments for $[Arg + M]^+$ (M = H, Li, Na, and K) were made by comparing measured action spectra to corresponding spectra measured for cationized arginine methyl ester $[ArgOMe + M]^+$ (M = H, Li, and Na) and absorbance spectra calculated for candidate structures. On the basis of spectral trends and the assignments of characteristic N−H stretches, the authors concluded that lithiated Arg favors a charge-solvated structure, whereas sodiated Arg is predominantly a salt-bridge isomer. These experiments were performed at elevated temperatures (404−470 K) using a heated vacuum chamber, so the stored ions have relatively high internal energies and undergo a limited extent of dissociation due to blackbody radiation alone. This enables photodissociation with as few as one photon, although multiple-photon processes may also contribute to the action spectra. As with all experiments conducted above 0 K and in which multiple photons can be absorbed prior to dissociation, additional higher-energy conformers may be present.

It is interesting to ask how cations other than alkali metals will be bound to arginine in the gas phase. The ionic radius of Ag^+ (1.2 Å) is larger than Na^+ (1.0 Å),[62] which suggests that SB structures might be favorable. However, Ag^+, having a $5s^04d^{10}$ electron configuration, can generally make shorter and more stable metal−ligand interactions than the closed-shell alkali-metal cations. In fact, Ag^+ binds more strongly to a single carbonyl ligand (89 kJ mol^{-1}) than either Li^+ (55 kJ mol^{-1}) or Na^+ (32 kJ mol^{-1});[63−65] this larger binding energy suggests a CS structure would be favored. Furthermore, Ag^+ binds even more strongly to nitrogen-containing ligands and is known to prefer a linear geometry,[66] suggesting that coordination to one or more nitrogen atoms is likely and that silver-bound arginine will adopt a charge-solvated conformation.

Here, we report IRMPD-action spectra in the 800−1900 cm^{-1} region for protonated arginine $[Arg + H]^+$ and arginine methyl ester $[ArgOMe + H]^+$ as well as the series of metal cationized arginine complexes, $[Arg + M]^+$ (M = Li, Na, K, Rb, Cs, and Ag), formed using ESI and measured using FT-ICR mass spectrometry and the Free Electron Laser for Infrared eXperiments (FELIX).[60] Charge-solvation structures are distinguished from salt-bridge structures based on the measured spectra. Conformational assignment is facilitated by comparison of measured spectra with those from electronic structure theory calculations.

Experimental Methods

Experiments were conducted using a 4.7 T FT-ICR mass spectrometer[36] constructed to permit IRMPD of ions in the cell by irradiation with FELIX.[60] The mass spectrometer is controlled using the Modular ICR Data Acquisition System (MIDAS)[67] while FELIX is controlled both at a central workstation and at a user terminal in the laboratory using LabVIEW software (National Instruments, Austin TX). Molecular ions of $[Arg + H]^+$, $[ArgOMe + H]^+$, the alkali-metal complexes $[Arg + Li]^+$, $[Arg + Na]^+$, $[Arg + K]^+$, $[Arg + Rb]^+$, and $[Arg + Cs]^+$, and $[Arg + Ag]^+$ were generated by infusing solutions composed in methanol/water (4:1 v/v) at a flow rate of ~10−45 μL min^{-1} into the ESI source (Z-spray, Micromass, Manchester, U.K.). Electrospray solutions were 1 mM Arg (Fluka, Buchs, Switzerland) or ArgOMe (Bachem AG, Bubendorf, Switzerland) with 1−5 mM metal salt adjusted to yield optimal signals for the metal complexes of interest. Metals were from hydroxide salts except Li^+ and Ag^+, which were derived from LiCl and $AgNO_3$ (Sigma, Zwijndrecht, The Netherlands), respectively. Ions were accumulated for 500 ms to 2 s in a storage hexapole prior to extraction through a quadrupole bender and a radio-frequency (RF)-octopole and finally into the Penning cell. Confinement of the ions was facilitated by an ion capture method described by Polfer et al.[43] Ion isolation was accomplished by use of a stored waveform inverse Fourier transform (SWIFT) as implemented in the MIDAS control software. For each complex investigated, care was taken to ensure that signals for any known fragment ions were eliminated during ion isolation. The FELIX beam (5−10 mm in diameter) used for IRMPD enters the vacuum chamber of the FT-ICR mass spectrometer through a ZnSe window and passes through the ion cloud multiple times by reflection from the polished Cu surface of the ICR cell plates.[43] Stored ions were irradiated with FELIX at a 5 Hz pulse rate for 1−3 s, corresponding to 5−15 macropulses. Macropulses (5 μs) consist of a series of micropulses (3 ps) separated by 1 ns having a peak output in the MW range to yield an average output on the order of 50 mJ/macropulse. The free electron laser was scanned in 0.01−0.05 μm increments (3−10 cm^{-1}), depending upon the subset of the wavelength range being scanned (12.5−5.25 μm/800−1900 cm^{-1}). Four IRMPD mass spectra were recorded at each IR wavelength. At wavelengths for which abundant fragmentation was observed, additional scans were performed with an attenuated beam to minimize saturation effects.

Signal transients were acquired from the mass spectrometer through a digital oscilloscope (Yokogawa DL4200, Tokyo, Japan) and further processed using LabVIEW modules to produce the IRMPD mass spectra. IR-action spectra were constructed by determining the fragmentation yield (yield) calculated from eq 1 at each IRMPD wavelength using the precursor (I_p) and fragment ion intensities (I_f)

$$\text{yield} = \frac{\sum_{f=1}^{n} I_f}{I_p + \sum_{f=1}^{n} I_f} \quad (1)$$

Action spectra shown in this report are constructed from multiple scans and are corrected linearly for laser power unless otherwise noted.

TABLE 1: Summary of the Conformational Searching Process and Ab Initio Calculations for the Cationized Arginine Species Examined in This Study

ion	no. MMFF structures	no. families identified	no. B3LYP optimized	no. MP2 optimized
$[Arg + H]^+$				
SB	25	5	9	
CS	85	22	40	
$[ArgOMe + H]^+$				
CS	77	14	26	
$[Arg + Li]^+$				
SB	48	15	39	
CS	145	15	35	
$[Arg + Na]^+$				
SB	69	15	41	6
CS (2)	205 + 125	15	109	5
$[Arg + K]^+$				
SB	78	15	29	
CS	389	15	33	
$[Arg + Rb]^+$				
SB	from Arg−K	15	25	
CS		15	32	
$[Arg + Cs]^+$				
SB	from Arg−Rb	15	25	
CS		15	26	
$[Arg + Ag]^+$				
SB	from Bush et al.[51]	7	7	
CS		4	4	

Computational Methods

The conformational landscape of protonated and alkali-metal cationized arginine complexes was explored using a combination of conformational searching with molecular mechanics force fields to identify candidate structures followed by electronic structure theory calculations to compute energies and vibrational spectra. The results of previous conformational explorations of our own[18,47,51] and others[4] were also considered to ensure that we had adequately explored the ions' potential energy surfaces (PESs). Salt-bridge and charge-solvated isomers were constructed and used as inputs for a Monte Carlo Multiple Minimum (MCMM) search carried out using MacroModel 8.1 (Schrödinger Inc., Portland, OR). For each isomer, 10 000 MCMM steps were performed, each followed by minimization using the Merck Molecular Force Field (MMFF94s).[68] Searches were carried out for CS isomers of $[ArgOMe + H]^+$ and SB and CS isomers of $[Arg + H]^+$, $[Arg + Li]^+$, $[Arg + Na]^+$, and $[Arg + K]^+$, yielding 25−389 unique conformers for each isomeric species (Table 1). Many of the conformers generated in the search are similar to other conformers found. Therefore, a sorting strategy was used to efficiently identify a subset of MMFF structures to explore the main features of the PES. MMFF conformers were grouped into conformational families using a homemade algorithm run with Matlab 7.0.4 (The Mathworks Inc., Mattick, MA). Briefly, the algorithm works by examining any of the possible noncovalent interactions (metal coordination and hydrogen bonds) that can be made in the energy-minimized structures. A logical matrix describing the conformational interactions of each structure is generated that is then used in a directed sorting process that sequentially groups conformers with similar interactions into families. Several candidate structures having low MMFF energy were selected for higher-level calculations from each conformer family to ensure adequate sampling of the large ensemble of structures. Candidate structures for the Rb^+ and Cs^+ complexes were generated from $[Arg + K]^+$ coordinate structures by replacement of the potassium cation with the larger metals. Starting structures for $[Arg + Ag]^+$ calculations came from additional conformation searching as well as the 10 lettered structures from Bush et al.[51]

TABLE 2: Precursor and Fragment Ions Contributing to the IR-Action Spectra

precursor ion		fragment ions (*m*/*z*)	
$[Arg + H]^+$	*m*/*z* 175	$-H_2O$	(157)
$[ArgOMe + H]^+$	*m*/*z* 189	$-NH_3$, −MeOH, −59, $[H_2N{=}C(NH_2)_2]^+$	(172, 157, 130, 60)
$[Arg + Li]^+$	*m*/*z* 181	$-H_2O$	(163)
$[Arg + Na]^+$	*m*/*z* 197	$-H_2O$	(179)
$[Arg + K]^+$	*m*/*z* 213	$-NH_3$, $-H_2O$, K^+	(196, 195, 39)
$[Arg + Rb]^+$	*m*/*z* 259	$-NH_3$, Rb^+	(242, 85)
$[Arg + Cs]^+$	*m*/*z* 307	$-NH_3$, Cs^+	(290, 133)
$[Arg + Ag]^+$	*m*/*z* 281/283	$-H_2O$, −60, −142, Ag^+	(263/265, 221/223, 139/141, 107/109)

Computations proceeded with hybrid method density functional theory (B3LYP) geometry optimizations and harmonic frequency analysis using the 6-31+G(d,p) basis set on all atoms (except rubidium, cesium, and silver for which the SDD Stuttgart/Dresden effective core potential[69] was used) as implemented in Gaussian 03.[70] Harmonic frequency calculations verified that all structures corresponded to local minima on the PES and provided zero-point energy (ZPE) and thermal corrections. Simulated IR spectra were constructed by scaling of harmonic frequencies by a factor of 0.98[33] followed by convolution with a Gaussian function using a full width at half-maximum of 20 cm^{-1}. Finally, single-point energy calculations were carried out at the MP2 level of theory using the larger 6-311++G(2d,2p) basis set. A summary of the conformation search and computation process is given in Table 1.

To determine whether relative energies computed from B3LYP geometry-optimized conformations agreed with more costly perturbation theory results, a subset of six low-energy SB and five low-energy CS conformers of sodiated arginine were geometry-optimized at the MP2 level of theory (6-31+G(d,p) basis set) followed by single-point energy calculations using the larger 6-311++G(2d,2p) basis set. MP2 optimization had little effect on relative conformational energies; for each of the nine conformers examined that were within 30 kJ mol^{-1} of the global minimum, the ZPE-corrected MP2 single-point relative energy computed at B3LYP- and MP2-optimized geometries differed by <2.5 kJ mol^{-1} (see the Supporting Information). All relative energies cited here were obtained from single-point MP2/6-311++G(2d,2p) calculations using the B3LYP/6-31+G(d,p)-optimized geometries with the exception of $[Arg + Na]^+$ for which the MP2-optimized geometries were used. (The single-point energy calculation (MP2/6-311++G(2d,2p)) using the B3LYP geometry failed to complete for the most important charge-solvated conformer of sodiated arginine (CS_A; see the Results section) due to excessive mixing of frozen core and valence orbitals. Thus, MP2/6-31+G(d,p) level optimized geometries were used to compare the relative stabilities of $[Arg + Na]^+$ conformers. A summary of all of the B3LYP and MP2 energies calculated for these 11 structures is included in the Supporting Information.) All reported energies are corrected for zero-point energy (derived from the B3LYP calculations) and are given relative to the global-minimum conformer, assigned a relative energy of $\Delta E_0 \equiv 0$ kJ mol^{-1}. Structures, relative energies, and computed spectra for all conformations considered may be found in the Supporting Information.

Energies and vibrational frequencies for $[Arg + Ag]^+$ complexes were also calculated by DFT using the 6-31+G(d,p) basis with the MPW1PW91 hybrid functional, which has been considered to give more reliable energetics of transition-metal complexes than the B3LYP functional.[37] The two functionals gave similar spectra, but B3LYP was chosen for spectral comparison for consistency with the alkali-metal complexes. Comparing the two functionals, B3LYP gave a noticeably better fit to the C=O stretching mode, which has shown particularly large computation-dependent variations and deviations in previous FELIX studies.

Results and Discussion

IRMPD-Action Spectroscopy. A summary of the precursor and product ions observed for each experiment is given in Table 2. The product ion spectra observed following IRMPD using FELIX were similar to those reported from CID and BIRD experiments[18] and IRMPD at shorter wavelengths.[51] However, in the previous studies K^+ was not observed as a product for $[Arg + K]^+$, and methanol loss was the only observed fragment for $[ArgOMe + H]^+$.[18,51] Additional fragment ion channels indicate that dissociation in these experiments can occur from highly activated precursor ions, although subsequent dissociation of fragment ions may also occur. Consistent with these previous studies, a change in the preferred dissociation pathway from loss of 18 Da (H_2O) to loss of 17 Da (NH_3) was observed to occur between the Na^+ and the K^+ complexes.

The IR-action spectra of the cationized arginine complexes are shown in Figure 1. It is immediately apparent that the spectra fall into three groups; the spectra for $[Arg + H]^+$ and $[ArgOMe + H]^+$ (Figures 1a and 1b) are strikingly similar to each other, as are those for $[Arg + Li]^+$ and $[Arg + Ag]^+$ (Figures 1c and 1h), as again are the spectra of $[Arg + Na]^+$, $[Arg + K]^+$, $[Arg + Rb]^+$, and $[Arg + Cs]^+$ (Figures 1d, 1e, 1f, and 1g). Similarity of the spectra in this region of the IR suggests similar heavy atom stretches (intense bands are primarily due to C−O and N−C stretches) as well as N−H and O−H bends; i.e., the similar spectral patterns suggest similar conformations.

The canonical (non-zwitterionic) form of Arg gives rise to a signature peak corresponding to the carbonyl stretching vibration (C=O) that should appear above 1700 cm^{-1}, well-separated from other modes of cationized arginine complexes that generally appear below 1700 cm^{-1}, or in the hydrogen stretch region (above 2500 cm^{-1}). In contrast, the salt-bridge isomers exhibit an asymmetric carboxylate (CO_2^-) stretch that is typically 75−100 cm^{-1} lower in wavenumber than a carbonyl stretch in simpler amino acids[33,35] and is expected to be shifted to an even lower wavenumber in Arg (discussed in further detail in the conformational assignment section). Other IR-active modes in this region are the intense N−H bending modes, located between 1500 and 1700 cm^{-1}, arising from both the N-terminal amino group and the guanidine side chain.

The protonated methyl ester of arginine (Figure 1a), which lacks an acidic proton and cannot form a zwitterion, exhibits a small band at 1750 cm^{-1} that is assigned to the C=O stretch. Note that the C=O stretch is clearly separated from the more intense band (arising from N−H bends) below 1700 cm^{-1}. The spectrum of protonated arginine (Figure 1b) shows remarkable similarity to $[ArgOMe + H]^+$ in the positions and relative intensities of both the main band at 1670 cm^{-1} and the smaller band at 1760 cm^{-1}, assigned to the C=O stretch. This provides

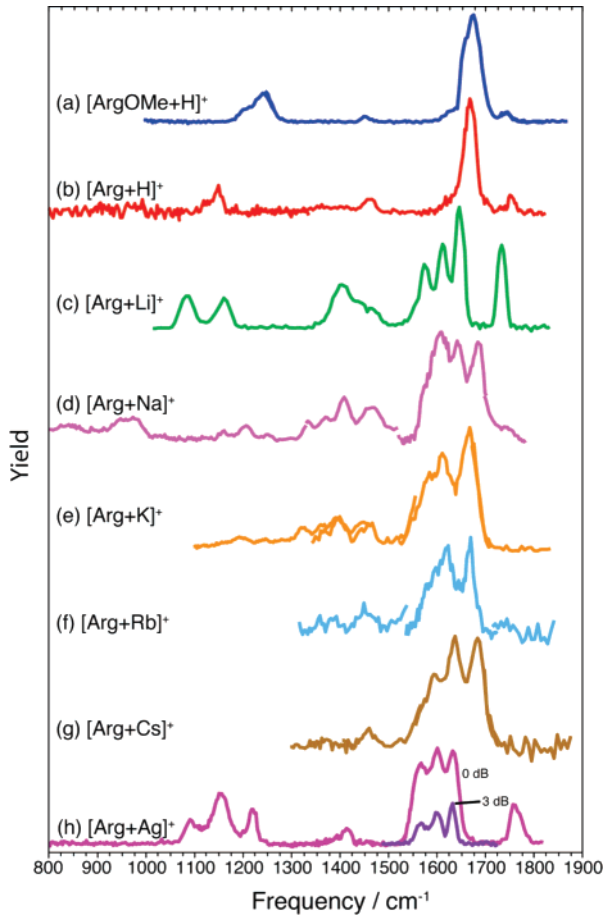

Figure 1. IRMPD-action spectra of arginine complexes measured using FELIX. For $[Arg + Ag]^+$, the action spectrum measured using the unattenuated FELIX beam is compared directly (no power correction for the attenuation) to that measured using 3 dB attenuation for the most intense bands.

strong evidence that $[Arg + H]^+$ must also exist in its canonical form. The band at ~1150 cm^{-1} is at the expected position for an O−H bend, also consistent with Arg being in its canonical form in $[Arg + H]^+$. The IR-action spectrum of $[Arg + Li]^+$ (Figure 1c) illustrates the effect that metal coordination has on the appearance of the mid-IR spectrum. The intense band at 1735 cm^{-1} is indicative of a carbonyl stretch; hence the lithiated arginine also appears to be a charge-solvated structure. The spectrum for $[Arg + Ag]^+$ (Figure 1h) is strikingly similar to that of $[Arg + Li]^+$. Assignment to a CS structure is strongly indicated by the prominent C═O stretching band at 1760 cm^{-1} and the characteristic O−H and N−H bending bands in the 1150 cm^{-1} region.

Figure 1d shows the measured spectrum of sodiated arginine. The intensity of the band above 1700 cm^{-1} is dramatically reduced (compared to $[Arg + Li]^+$), suggesting that sodiated arginine primarily exists as a salt bridge, although the presence of a small proportion of a charge-solvated conformer is possible. This prospect is discussed in further detail in the conformational assignment section. The IR-action spectra of the larger alkali-metal complexes (Figures 1e−g) are all very similar in the measured range. For K^+, Rb^+, and Cs^+ complexes, the spectra are devoid of any distinguishing feature above 1700 cm^{-1}, thus indicating that these Arg complexes have salt-bridge structures. Furthermore, the spectra for $[Arg + M]^+$ (M = Na, K, Rb, and Cs) all exhibit intense bands at ~1680 cm^{-1} that are not present in the spectra for M = Li and Ag, supporting the preliminary assignment of these groups of complexes to (at least) two different structural families.

The series of spectra shown in Figure 1 provide convincing evidence that $[ArgOMe + H]^+$, $[Arg + H]^+$, $[Arg + Li]^+$, and $[Arg + Ag]^+$ can be assigned to charge-solvated conformations because of the existence of the signature carbonyl stretches in the mid-IR region. Furthermore, this series of IRMPD-action spectra provide clear spectroscopic evidence for the transition from a charge-solvated conformation to a salt-bridge conformation as the size of the coordinating alkali metal is increased, in agreement with conclusions of Jockusch et al.[18] based on trends in dissociation behavior and computed relative energies and on those of Bush et al.[51] based on spectroscopy of the hydride stretching region. It is interesting to note that despite the preference for $[Arg + Na]^+$ to dissociate by loss of H_2O[18] and kinetic method results that suggest arginine exists as a CS conformer in the sodium-bound heterodimer of Arg and ArgOMe,[27] the spectroscopic evidence points strongly toward sodiated arginine existing primarily in a salt-bridge conformation. The apparent discrepancy between ion structure and reactivity is likely due to the barriers for structural isomerization and for the loss of a water molecule from the non-zwitterionic form being lower than that for the loss of ammonia from the zwitterionic form.[51]

Computations. The lowest-energy CS and lowest-energy SB conformer for each cationized Arg complex are shown in Figure 2, together with the two most stable CS conformers of $[ArgOMe + H]^+$. Additional structures and energies considered for each complex are included in the Supporting Information. The results of these calculations agree with conclusions based on the spectroscopic evidence alone; i.e., charge-solvated complexes are computed to be the most stable for $[Arg + H]^+$, $[Arg + Li]^+$, and $[Arg + Ag]^+$, while salt-bridge complexes are the most stable for $[Arg + M]^+$ (M = Na, K, Rb, and Cs).

Despite the large number of local minima on the PES considered for each complex (Table 1 and the Supporting Information), a single structure from the ensemble of SB conformers (SB_D) and only three structures from the CS families (CS_A, CS_L, and CS_M) were consistently found to be the most stable for the metal cation complexes. In SB_D, the metal ion is coordinated to the (formally negatively charged) carboxylate group. Additional stabilization is provided by hydrogen bonds present between the terminal N^{η}−H of the side chain and the carboxylate oxygen and between the internal N^{ϵ}−H of the side chain and N^T. This latter interaction provides a spectral signature for the SB complexes. This band is not present in any of the metal complex CS structures (though it is present in the protonated structures), which all have the N^{ϵ}−H pointing away from the rest of the complex. The perturbed N^{ϵ}−H(···O) bend is computed to lie at higher wavenumber (~1680 cm^{-1}) than other N−H bends of the side chain and the N-terminal amino group (see below).

The favored mode of metal ion coordination in CS complexes depends on the metal ion (Figure 2 and Table 3). Lithium, sodium, and potassium complexes (CS_A) are tri-coordinate, with the metal ion in close proximity to the carbonyl oxygen, N^{η} of the side chain, and the N-terminal amino group. The larger alkali-metal complexes (CS_L) prefer a different tri-coordinate geometry, the metal interaction with N^{η}, $N^{\eta'}$, and the carbonyl oxygen, with the N^T accepting a hydrogen bond from the terminal hydroxyl group rather than chelating the metal ion. Finally, the $[Arg + Ag]^+$ complex features di-coordination of the metal ion; in CS_M, the silver cation is coordinated to N^{η} of the side chain and N^T but lacks a significant interaction with

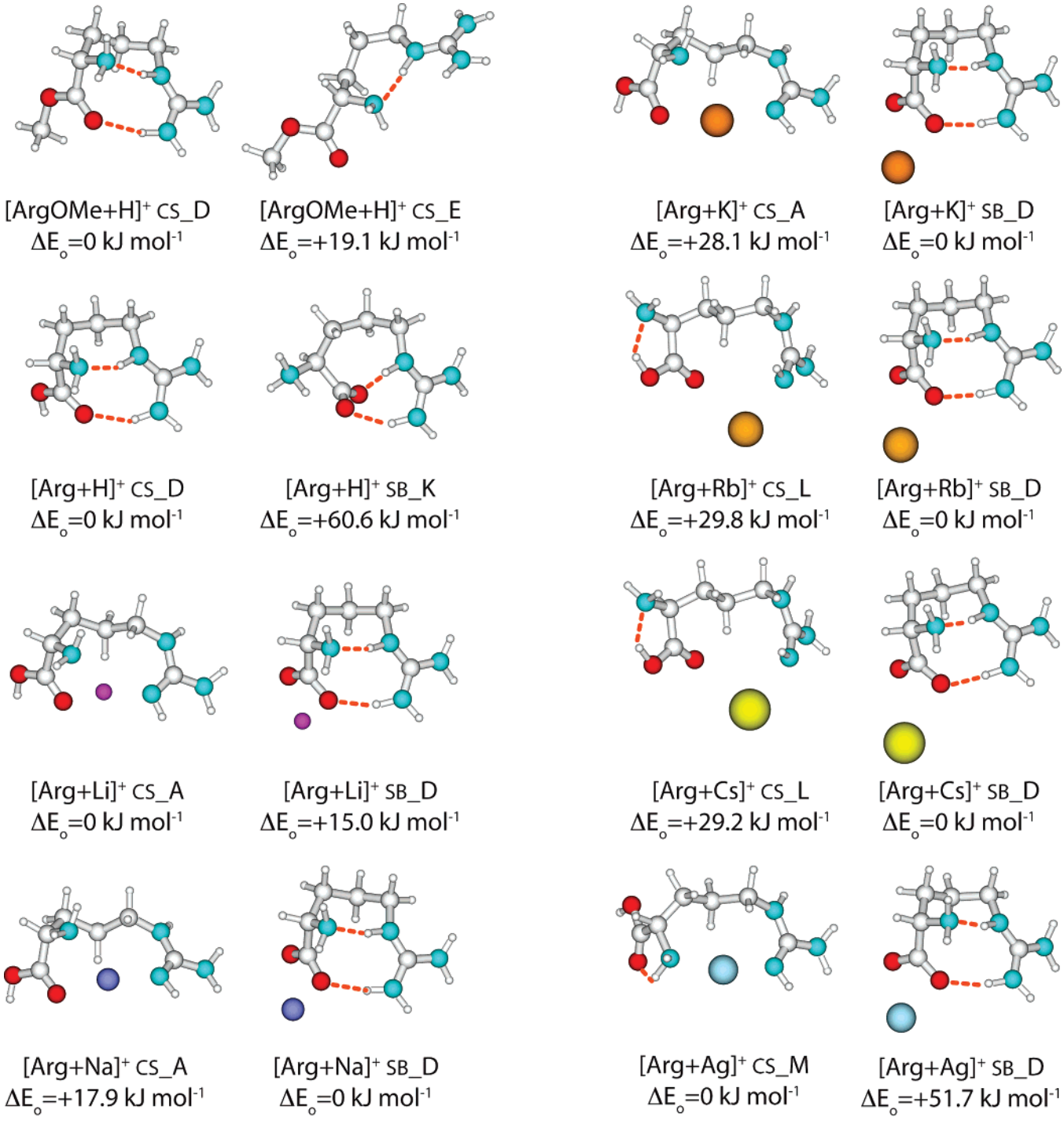

Figure 2. Low-energy charge-solvated and salt-bridge conformers of the Arg species for geometries calculated at the B3LYP/6-31+G(d,p) level of theory with relative energies taken from ZPE-corrected, single-point MP2/6-311++G(2d,2p) calculations.

TABLE 3: Arginine−Metal Ion Binding Distances (Å) for the Minimum-Energy Charge-Solvated and Salt-Bridge Conformers

		charge-solvated						salt-bridge	
		C=O	HO	N^T	N^η	$N^{\eta'}$		$COO^{-\prime}$	$COO^{-\prime\prime}$
$[Arg + Li]^+$	CS_A	1.97	3.95	2.12	1.94	4.25	SB_D	1.87	1.94
$[Arg + Na]^+$	CS_A	2.30	4.32	2.48	2.30	4.63	SB_D	2.21	2.30
$[Arg + K]^+$	CS_A	2.67	4.76	2.97	2.73	5.09	SB_D	2.57	2.73
$[Arg + Rb]^+$	CS_L	2.80	4.48	6.21	2.97	3.45	SB_D	2.76	2.94
$[Arg + Cs]^+$	CS_L	2.99	4.63	6.41	3.18	3.70	SB_D	2.92	3.16
$[Arg + Ag]^+$	CS_M	3.89	4.91	2.19	2.12	4.35	SB_D	2.25	2.51

the carbonyl oxygen. Note that CS_A is not a local minimum on the B3LYP/6-31+G(d,p) PES for $[Arg + Ag]^+$ though it is at the B3LYP/DZVP level of theory.[71] At the B3LYP/6-31+G-(d,p) level, CS_M results from geometry optimization of CS_A after substitution of Ag^+ for Li^+. Likewise, CS_M is not a local minimum on the PES of lithiated arginine; substitution of Li^+ for Ag^+ in CS_M followed by geometry optimization results in CS_A. The difference in coordination geometry between the

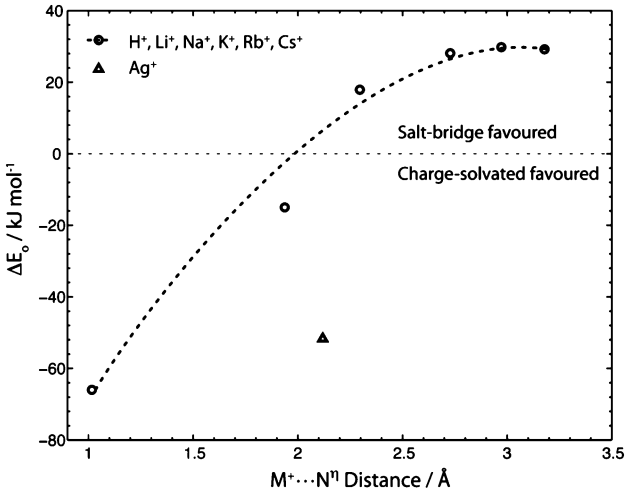

Figure 3. Correlation between cation−ligand bond distances and relative stability of the lowest-energy CS conformers with respect to the lowest-energy SB conformers for the seven $[Arg + M]^+$ species (M = H, Li, Na, K, Rb, Cs, and Ag). The dotted line serves as a guide to the eye, illustrating the trend among group 1 elements.

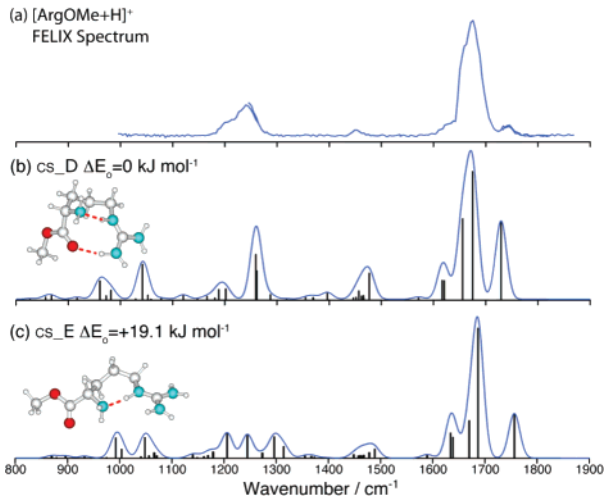

Figure 4. (a) IR-action spectrum of $[ArgOMe + H]^+$ measured using FELIX and calculated spectra for two low-energy conformers (b) CS_D and (c) CS_E.

alkali-metal ions and silver is consistent with the known preference of Ag to bind N over binding O.[66,72,73] Additionally, Ag^+ prefers linear ligand−Ag−ligand complexes.[73]

Figure 3 shows the relationship between metal ion size (taken to be the $M^+\cdots N^\eta$ interaction distance in the CS structures) and relative stability of the SB and CS structures for each $[Arg + M]^+$ complex investigated in this work. While the correlation between alkali-metal ion size and relative stability of salt-bridge structures has been noted previously,[18,51] it is clear that $[Arg + Ag]^+$ deviates from this trend. The increased relative stability calculated for charge-solvated $[Arg + Ag]^+$ complexes is another illustration of the strong affinity Ag^+ has for nitrogen-containing ligands.[66]

A comparison of the low-energy conformers of protonated Arg identified in our search with those recently reported by Ling et al.[4] gives us added confidence in our conformational search procedure and computational methods. Six low-energy CS conformers computed at the CCSD//MP2/6-31++G(d,p) level of theory were reported by the authors, each of which was identified independently in our search. Moreover, the two most stable structures identified in our calculations are the same as those of Ling et al., and the calculated relative energy differences between the two structures is virtually the same: 7.9 kJ mol^{-1} (Ling et al.) versus 8.2 kJ mol^{-1} (this work).

For all of the Arg−metal ion complexes studied here, several minima were identified within 20 kJ mol^{-1}, and at least one similar structure was typically located within 10 kJ mol^{-1} (Supporting Information). Thus, under the experimental conditions employed here, it is possible that more than one conformation is significantly populated and contributes to the IRMPD spectrum. However, similar conformers (for example, those within the same family based on primary stabilizing interactions) may not be distinguishable in the mid-IR region because of the similarity of the interactions. Nevertheless, some conformational assignments may be made based on the comparison of measured and computed spectra.

Assignment of Structures. There are several considerations concerning matching simulated spectra to measured spectra, which have been discussed in detail elsewhere.[33,38,41,43] B3LYP harmonic vibrational frequencies are typically overestimates due to deficiencies in the computation method that result in calculated covalent bond lengths that are slightly too long and because of anharmonicities present in real PESs. IRMPD-action spectra are also known to exhibit a degree of red-shifting due to the multi-photon nature of the IRMPD process in conjunction with anharmonicities.[53] To account for these phenomena when comparing spectra, computed frequencies are often scaled to better reflect the measured spectra. Various scaling factors have been proposed, the magnitude of which depend upon the wavelength range under investigation and the level of theory used in the calculations. In this case, a scaling factor of 0.98 has been adopted, the same scaling factor used by Kapota et al.[33] in a spectroscopic and computational investigation of amino acid−metal complexes employing the same level of theory used here for frequency calculations.

A further consideration when matching spectra concerns the relative intensities of measured bands. While relative intensities generally show a close to linear dependence on power, exceptions can occur. These have been discussed in more detail elsewhere.[40,52,53] Vibrational modes, particularly those having large absorption cross-sections, may be saturated during the multi-photon absorption process. Because the apparent absorption intensity is measured as a function of fragmentation efficiency (yield), the apparent absorption intensities of some peaks may be significantly underestimated (by as much as a factor of 2 or more),[43,52] and spectra may additionally be prone to band broadening. At irradiation wavelengths resulting in highly efficient fragmentation, the FELIX beam was attenuated to alleviate excessive band broadening and to improve the reliability of intensity information. An additional concern is that the absorption on excited-state surfaces may be different than ground-state absorption (as, for example, in the case where a change in geometry alters the absorption cross-section). Thus, while matching band appearances based upon peak intensities is often satisfying, peak position and peak spacing is believed to be a more reliable approach for matching spectra.

$[ArgOMe + H]^+$ and $[Arg + H]^+$. $[ArgOMe + H]^+$ can adopt only a CS-type structure and was measured to provide a model with which to compare subsequent arginine complexes. Two low-energy conformers whose simulated spectra best match the measured spectrum are shown in Figure 4, CS_D (ΔE_0 = 0 kJ mol^{-1}) and CS_E (ΔE_0 = +19.3 kJ mol^{-1}). The computed spectra both exhibit intense bands at 1650−1700 cm^{-1} due to N−H bends and an additional diagnostic peak at 1750 cm^{-1} corresponding to the C=O stretch in the simulated spectra. The intensity of the measured C=O stretch is significantly lower

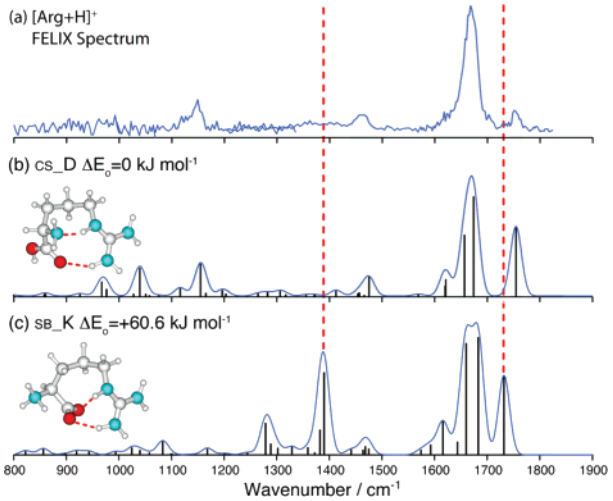

Figure 5. (a) IR-action spectrum of $[Arg + H]^+$. Simulated IR spectra of (b) the minimum-energy CS conformer and (c) the minimum-energy salt-bridge conformer SB_K. Defining features ruling out the presence of SB_K are shown with the dashed lines.

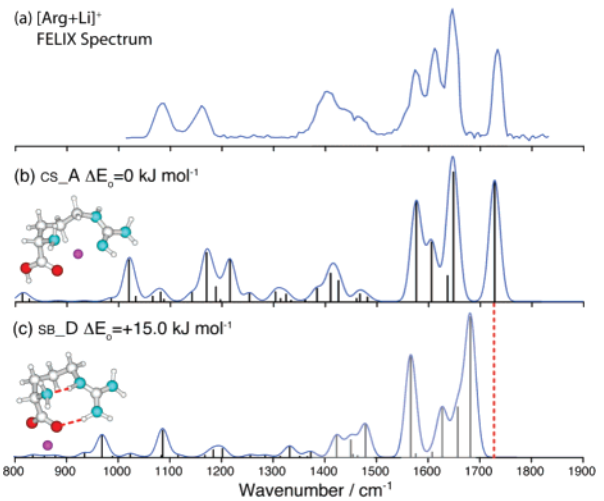

Figure 6. (a) IR-action spectrum of $[Arg + Li]^+$. Simulated IR spectra of (b) the minimum-energy CS conformer and (c) the minimum-energy SB conformer.

than predicted by the calculations. Weaker than predicted intensities for carbonyl stretching bands have also been observed for other molecules.[52] Possible explanations for this discrepancy include: (1) low FELIX power in this range combined with a nonlinear power dependence of band intensities, (2) anharmonicity in this mode may be somewhat larger than average, resulting in a reduced excitation efficiency, (3) deficiencies in the computations resulting in overprediction of the dipole moment derivative, (4) a change in conformation during the excitation to a structure with a somewhat different carbonyl stretching frequency, and (5) saturation of the transition during the multi-photon excitation process, resulting in a weaker apparent band intensity.

Comparing the measured and simulated spectra of $[Arg + H]^+$ shown in Figure 5, it is immediately clear that the minimum-energy conformer, CS_D, is a very good match to the measured spectrum. The low-energy conformers of both $[ArgOMe + H]^+$ and $[Arg + H]^+$ are from the same structural family. It is therefore not surprising that their computed spectra also share many features, as do the measured spectra for the protonated species. Notably, the signature carbonyl stretch ($\sim$1750 cm^{-1}) appears to be very similar to that measured for the methyl ester, also showing a much lower intensity than predicted by calculation. In addition, the intense bands between 1600 and 1700 cm^{-1} and the small band at $\sim$1450 cm^{-1}, corresponding to multiple N−H bending modes coupled to C−N stretches, have similar widths and relative intensities in the two measured spectra. The band at 1150 cm^{-1} is assigned to the O−H bend for the CS $[Arg + H]^+$. In the protonated methyl ester, this band is replaced by one appearing at $\sim$1250 cm^{-1} corresponding to the O−CH_3 bend.

For comparison, the simulated spectrum of the lowest-energy salt-bridge conformer of $[Arg + H]^+$ (SB_K) is shown in Figure 5c. The difference in relative stabilities at the MP2 level of theory between CS_D and SB_K is large ($\Delta E_0 = 60.6$ kJ mol^{-1}), sufficiently so that the presence of the salt-bridge isomer can likely be ruled out based on this energy gap alone. Significant population of the salt-bridge structure for protonated arginine can also be ruled out based on the lack of peaks at 1390 and 1730 cm^{-1} in the experimental spectrum (dotted lines on figure), which would arise from coupled N−H bending modes of the protonated N-terminal amino group and the carboxylate stretch of the salt-bridge conformer.

$[Arg + Li]^+$. The measured spectrum of $[Arg + Li]^+$ together with the lowest-energy CS and lowest-energy SB conformers are shown in Figure 6. The match to CS_A, the global minimum, is very good. In particular, CS_A features an intense carbonyl stretch at 1730 cm^{-1}, a band that is present in the experimental spectrum. The relative intensity of the carbonyl stretch band of $[Arg + Li]^+$ appears better reproduced by the calculated spectrum than that of the protonated species discussed above. A further difference from the protonated species is the appearance of the N−H bends. In $[Arg + Li]^+$, these appear as a distinct triplet of bands spanning the range of 1550−1650 cm^{-1}, compared to the narrower band observed at a somewhat higher wavenumber for the protonated species. The lowest-energy feature of the triplet of bands, calculated to lie at $\sim$1575 cm^{-1} in CS_A, corresponds to the N^{ϵ}−H bend; this group points away from the metal binding pocket in $[Arg + Li]^+$ CS_A, while in the lithiated SB (and protonated) complexes the N^{ϵ}−H bending mode is perturbed by hydrogen bonding to the N-terminal amino group and lies at a higher wavenumber, $\sim$1680 cm^{-1}. The appearance of these key features is predicted well in the computed spectrum of the global-minimum structure, CS_A, and $[Arg + Li]^+$ is therefore assigned to this conformation.

The simulated spectrum of the lowest-energy salt-bridge conformer (SB_D) is shown for comparison in Figure 6c. The relative stability of SB_D ($\Delta E_0 = +15.0$ kJ mol^{-1}) is much closer to the global minimum than for protonated arginine but would not be significantly populated at room temperature if the computed relative energies are correct. Indeed, the computed spectrum of SB_D does not suitably match the measured IRMPD spectrum. In particular, the spacing between the asymmetric CO_2^- stretch (1570 cm^{-1}) and the highest-energy intense N−H bend (N^{ϵ}−H, 1680 cm^{-1}) is inconsistent with the measured spectrum, which exhibits a separation of only $\sim$75 cm^{-1} between the outer features of the triplet, indicating little or no population of this salt-bridge structure. The matches with higher-energy salt-bridge structures are equally poor (Supporting Information).

$[Arg + Na]^+$. The IRMPD-action spectrum of sodiated arginine along with the spectra of three possible SB conformers and one CS conformer are shown in Figure 7. The global-minimum structure is a salt bridge (SB_D), and the calculated spectrum for SB_D matches the measured $[Arg + Na]^+$ spectrum quite well over the entire range probed, while the CS structures do not provide a good match. Also shown in Figure 7 is the

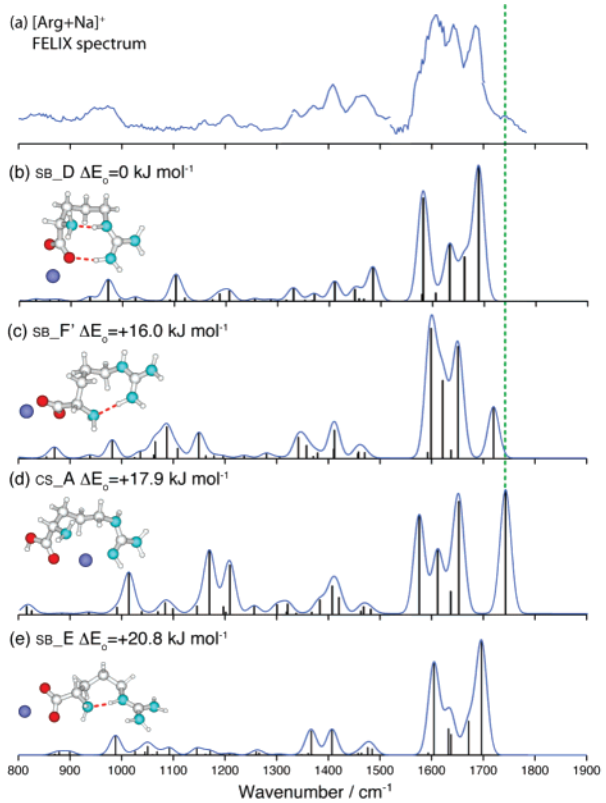

Figure 7. (a) IR-action spectrum of $[Arg + Na]^+$. Simulated IR spectra of (b) the minimum-energy SB conformer, (c) an alternative SB conformer SB_F′, (d) the minimum-energy CS conformer CS_A, and (e) SB_E.

simulated mid-IR spectrum of a higher-energy conformer, SB_E, which provides a better match to the measured IR-action spectrum in the hydrogen stretch region (2600−3800 cm^{-1}) than does SB_D.[51] The calculated mid-IR spectra of SB_D and SB_E are quite similar, and both match the measured spectrum well. Both conformers feature a N^{ϵ}−H that donates a hydrogen bond to the N-terminal amino group, resulting in an intense N^{ϵ}−H bending mode at ∼1690 cm^{-1}, a band observed in the measured spectrum of $[Arg + Na]^+$ and that is absent from the measured spectrum of $[Arg + Li]^+$. Thus, we are not able to distinguish between these possible SB conformations based on the mid-IR results, though the relatively high relative energy of SB_E (+21 kJ mol^{-1}) at the MP2/6-311++G(2d,2p)//MP2/6-31+G(d,p) level of theory used in this work compared to its B3LYP/6-31++** calculated energy (+9 kJ mol^{-1})[51] makes it a less likely assignment. Despite not being able to make a clear conformational assignment among salt-bridge structures, the appearance of a band at ∼1690 cm^{-1}, combined with the significant decrease in intensity of the band assigned to the carbonyl stretch, provides strong evidence that $[Arg + Na]^+$ exists predominately as a salt-bridge complex under our experimental conditions.

The measured spectrum exhibits a low-intensity (yet reproducible) band at ∼1745 cm^{-1} that is not predicted for SB_D or SB_E. This band falls in the same region as the C═O stretches previously assigned to a charge-solvated structure of $[Arg + Li]^+$; thus it suggests the existence of a small population of CS structures of $[Arg + Na]^+$. Note that it is highly unlikely that the band at 1745 cm^{-1} results from an isomerization of a SB conformer to a CS conformer induced by the 1−3 s of laser irradiation. In principle, it is possible that different structures can isomerize upon IR activation. However, this can only happen if both structures absorb at the same wavelength. In this case, the band at 1745 cm^{-1} appears where the SB conformers do not display an absorption band.

A likely candidate for the distinct population that produces this band is the lowest-energy charge-solvation conformer (CS_A), for which the carbonyl stretch is predicted at 1740 cm^{-1}, very near the measured position (1745 cm^{-1}). CS_A is calculated to be 17.9 kJ mol^{-1} higher in energy than SB_D; thus, if the band at 1745 cm^{-1} is due to the population of CS structures, then this indicates that calculations at the level of theory used here underestimate the stability of CS complexes. The intensity of this peak is clearly quite low in contrast to the much more intense peak measured for lithiated arginine. Therefore, the relative abundance of any CS structures appears to be low.

Alternatively, the band at 1745 cm^{-1} could be due to the existence of a second zwitterionic conformer illustrated in Figure 7c (SB_F′), which has a band at ∼1720 cm^{-1} (corresponding to a N^{η}−H bend of the guanidino side chain blue-shifted by a hydrogen bond to the N-terminal amino group). This alternative SB conformer lies at $\Delta E_0 = +16.0$ kJ mol^{-1}, slightly lower in energy than CS_A. The mid-IR results alone do not allow us to distinguish between these possibilities. However, photodissociation spectra measured in the hydrogen stretching region by Bush et al.[51] rule out significant population of SB_F. Instead, the authors concluded that the population of sodiated arginine consisted of roughly 90% salt-bridge and 10% charge-solvated conformers. This mixture of SB and CS conformers would also account adequately for the appearance of the mid-IR-action spectrum of sodiated Arg.

$[Arg + K]^+$, $[Arg + Rb]^+$, and $[Arg + Cs]^+$. The IRMPD-action spectra of the larger alkali-metal complexes closely resemble each other and all match well the computed spectra for the global-minimum conformer for each of these complexes, SB_D (Figure 8). The absence of a carbonyl stretching band and the presence of a band at ∼1690 cm^{-1} corresponding to a hydrogen-bonded N^{ϵ}−H bend support assignment of $[Arg + K]^+$, $[Arg + Rb]^+$, and $[Arg + Cs]^+$ to SB structures. In addition, the similarity of the measured spectra among which both the spacing and the position of the most intense bands (1550−1700 cm^{-1}) are virtually unchanged suggest assignment to the same conformer or family of conformers. The $[Arg + K]^+$ spectrum exhibits similar features between 1300 and 1500 cm^{-1} to those of the $[Arg + Na]^+$ spectrum. In addition, the $[Arg + K]^+$ spectrum has good signal-to-noise ratio above 1700 cm^{-1}, and unlike the sodiated spectrum, there is no evidence of a C═O stretching band for the potassiated complex. Finally, given the large energy differences between the lowest-energy CS conformer and the global minimum for each complex (charge-solvation structures lie at $\Delta E_0 = +28.1$, +29.8, and +29.2 kJ mol^{-1} for K^+, Rb^+, and Cs^+, respectively (Figure 2)), the evidence for assignment of the SB structure is compelling. This is consistent with the deconvolution of the higher-frequency IRMPD spectrum of $[Arg + K]^+$, which provided no evidence for charge-solvated structures of this ion.[51]

Population of zwitterionic conformers other than SB_D cannot be ruled out. The next most stable SB structures for K^+, Rb^+, and Cs^+ are at +7.0, +7.2, and +6.7 kJ mol^{-1} (Supporting Information). These structures are in the same conformational family as SB_D, exhibiting the same important binding interactions with the metal ion and differing primarily by torsional angles of the alkyl portion of the side chain. Population of SB_E, the conformer whose IR-action spectrum in the hydrogen stretch region agrees well for $[Arg + Na]^+$ and $[Arg + K]^+$ (see previous section)[51] is similarly a possibility; this conformer lies at +19.8 kJ mol^{-1} for $[Arg + K]^+$ and exhibits many of the

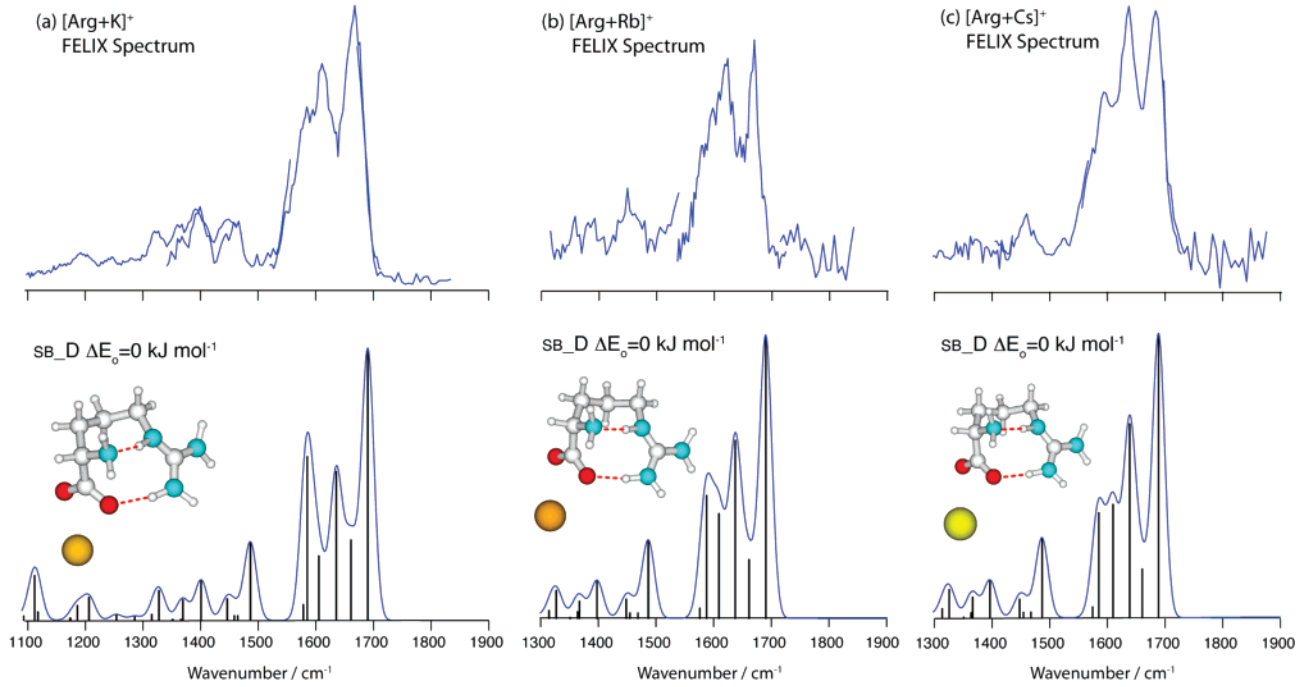

Figure 8. IR-action spectra and simulated vibrational spectra for (a) [Arg + K]$^+$, (b) [Arg + Rb]$^+$, and (c) [Arg + Cs]$^+$.

same interactions as SB_D (Figure 7). The computed spectra for these alternative SB structures and those of SB_D are virtually indistinguishable in the 1300−1900 cm^{-1} region.

[Arg + Ag]$^+$. Figure 9 shows the IRMPD-action spectrum of [Arg + Ag]$^+$. At first glance, it is strikingly similar to that of [Arg + Li]$^+$. The region with the most intense bands (1550−1650 cm^{-1}) was also scanned with an attenuation of 3 dB, as shown in red. Also shown are calculated spectra of three low-energy CS structures and two SB structures. The fit between the observed spectrum and the lowest-energy structure (CS_M) is very good, with six matching features indicated. Conformer CS_C also shares a number of similarities with the measured spectrum although the match is not as good as CS_M, and the significantly lower stability of this structure (+22.0 kJ mol^{-1}) makes it much less attractive.

Assignment to a CS structure is strongly indicated by the prominent C═O stretching band at 1755 cm^{-1} and the characteristic OH and NH bending bands in the 1150 cm^{-1} region. A SB structure with zwitterionic Arg would show the characteristic carboxylate peak around 1535 cm^{-1} and a N$^{\epsilon}$−H bend around 1680 cm^{-1}, neither of which is present in the spectrum. Therefore, anything more than a very small fraction of zwitterions in the population can be ruled out. Among the CS structures, it is clear that only structures with Ag$^+$ chelated to two nitrogen atoms (CS_M and CS_C) are possible, the carbonyl oxygen/N$^{\eta}$ chelation of CS_B being clearly ruled out. As discussed in the computational results subsection, the metal coordination of CS_M and CS_C differs from CS_A (assigned for [Arg + Li]$^+$). Additional evidence for different coordination geometries comes from the multiple minor differences between the measured spectra of [Arg + Li]$^+$ and [Arg + Ag]$^+$. These differences include: (1) a small shift in the band assigned to the carbonyl stretch (1735 cm^{-1} in the Li$^+$ complex versus 1755 cm^{-1} in the Ag$^+$ complex), (2) the appearance of the spectrum between 1000 and 1300 cm^{-1}, which shows two distinct features for the Li$^+$ complex but three for the Ag$^+$ complex, and (3) the appearance of the band around 1400 cm^{-1}, which is broad and relatively intense for the Li$^+$ complex and less so for the Ag$^+$ complex. The appearance of these minor features is reproduced very well in the calculated spectra of CS_M for [Arg + Ag]$^+$ and CS_A for [Arg + Li]$^+$, with the exception of the 1000−1300 cm^{-1} region for CS_A.

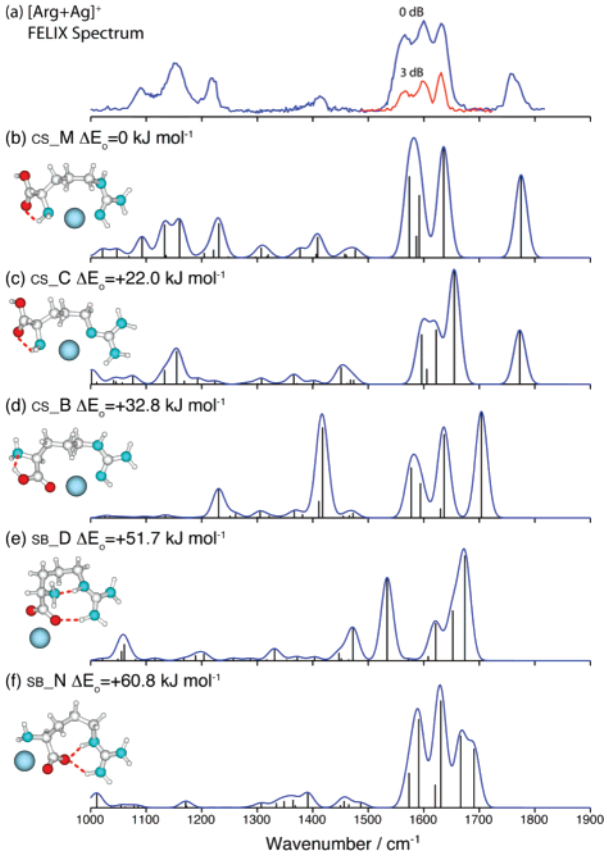

Figure 9. (a) IR-action spectrum of [Arg + Ag]$^+$ and (b−f) the computed vibrational spectra of three low-energy CS and two low-energy SB conformers. Relative energies are from ZPE-corrected, single-point calculations on the B3LYP geometries at the MP2 level of theory (6-311++G(2d,2p) basis set, using the SDD effective core potential for Ag$^+$.

Conclusions

IR-action spectroscopy has been used to measure the spectra of $[ArgOMe + H]^+$ and $[Arg + M]^+$ (M = H, Li, Na, K, Rb, Cs, and Ag) using IRMPD in an FT-ICR mass spectrometer. Charge-solvated conformations are readily distinguished from the salt-bridge isomers, based on their signature spectra in the range of 800−1900 cm^{-1}. The measured spectrum of $[ArgOMe + H]^+$ identified a diagnostic peak corresponding to the C═O stretch that is indicative of the CS conformation. A similar signature peak was observed for protonated, lithiated, and silver-bound Arg, providing strong evidence that these complexes also exist in CS conformations. The larger alkali-metal cation complexes (K^+, Rb^+, and Cs^+) exhibit spectra consistent with a SB conformation, showing no trace of the diagnostic C═O stretch above 1700 cm^{-1} and exhibiting a band at ∼1690 cm^{-1} that is assigned to the $N^{\epsilon}\cdots H$ bend, which is perturbed by a hydrogen bond to the N-terminal amino group. For $[Arg + Na]^+$, the IR-action spectrum indicates that the ion population is predominantly made up of SB conformers. However, a small peak observed at 1745 cm^{-1} suggests a small population of CS conformers. The structural conclusions from the data for protonated, lithiated, sodiated, and potassiated complexes are in agreement with those reported by Bush et al.[51] based on spectroscopic measurements in the O−H and N−H stretching region of the spectrum (2500−3800 cm^{-1}). The conformation of $[Arg + Ag]^+$ assigned here to a CS structure differs from the alkali-metal cationized Arg complexes; calculations show that Ag^+ is di-coordinated to Arg, interacting with nitrogen atoms of both the N-terminal amino group and side chain while $[Arg + Li]^+$ is tri-coordinated, with an additional metal−carbonyl oxygen interaction.

The conformational landscape of each arginine-based complex was extensively explored using a combination of conformation searching in conjunction with molecular mechanics followed by electronic structure theory calculations. Conformational assignments for each complex have been made by matching simulated spectra of low-energy conformers to measured spectra. In each case examined here, the measured spectra matched well the spectra calculated for the global-minimum conformers.

Acknowledgment. This work is part of the research program of FOM, which is financially supported by the Nederlandse Organisatie voor Wetenschappeklijk Onderzoek. Construction and shipping of the instrument and also travel of R.C.D. and R.A.J. for the present project were made possible with funding from the National High Field FT-ICR Facility (Grant No. CHE-9909502) at the National High Magnetic Field Laboratory, Tallahassee, FL. Additional financial support was provided by the Natural Sciences and Engineering Research Council (M.W.F. and R.A.J.), the Canada Chairs Program (R.A.J.), and the National Science Foundation (Grant No. CHE-0415293 (E.R.W.)). The skillful assistance of the FELIX staff is gratefully acknowledged.

Supporting Information Available: For each complex examined, tables listing electronic energies and thermal corrections for all candidate conformations, pictures of the conformations, and computed spectra. This material is available free of charge via the Internet at http://pubs.acs.org.

References and Notes

(1) Alberts, B.; Johnson, A.; Lewis, J.; Raff, M.; Roberts, K.; Walter, P. *Molecular Biology of the Cell*, 4th ed.; Garland Science: New York, 2002.

(2) Kassab, E.; Langlet, J.; Evleth, E.; Akacem, Y. *J. Mol. Struct.: THEOCHEM* **2000**, *531*, 267.

(3) Hunter, E. P.; Lias, S. G. Proton affinity evaluation In *NIST Chemistry WebBook*; Linstrom, P. J., Mallard, W. G., Eds.; NIST Standard Reference Database 69; National Institute of Standards and Technology: Gaithersburg MD, 2005.

(4) Ling, S. L.; Yu, W. B.; Huang, Z. J.; Lin, Z. J.; Haranczyk, M.; Gutowski, M. *J. Phys. Chem. A* **2006**, *110*, 12282.

(5) Wyttenbach, T.; Witt, M.; Bowers, M. T. *J. Am. Chem. Soc.* **2000**, *122*, 3458.

(6) Julian, R. R.; Jarrold, M. F. *J. Phys. Chem. A* **2004**, *108*, 10861.

(7) Lemoff, A. S.; Bush, M. F.; O'Brien, J. T.; Williams, E. R. *J. Phys. Chem. A* **2006**, *110*, 8433.

(8) Lemoff, A. S.; Bush, M. F.; Williams, E. R. *J. Phys. Chem. A* **2005**, *109*, 1903.

(9) Lemoff, A. S.; Bush, M. F.; Williams, E. R. *J. Am. Chem. Soc.* **2003**, *125*, 13576.

(10) Bush, M. F.; Forbes, M. W.; Jockusch, R. A.; Oomens, J.; Polfer, N. C.; Saykally, R. J.; Williams, E. R. *J. Phys. Chem. A* **2007**, *111*, 7753.

(11) Jockusch, R. A.; Lemoff, A. S.; Williams, E. R. *J. Am. Chem. Soc.* **2001**, *123*, 12255.

(12) Jockusch, R. A.; Lemoff, A. S.; Williams, E. R. *J. Phys. Chem. A* **2001**, *105*, 10929.

(13) Aikens, C. M.; Gordon, M. S. *J. Am. Chem. Soc.* **2006**, *128*, 12835.

(14) Remko, M.; Rode, B. M. *J. Phys. Chem. A* **2006**, *110*, 1960.

(15) Lemoff, A. S.; Wu, C. C.; Bush, M. F.; Williams, E. R. *J. Phys. Chem. A* **2006**, *110*, 3662.

(16) Xu, S. J.; Nilles, M.; Bowen, K. H. *J. Chem. Phys.* **2003**, *119*, 10696.

(17) Wyttenbach, T.; Witt, M.; Bowers, M. T. *Int. J. Mass Spectrom.* **1999**, *183*, 243.

(18) Jockusch, R. A.; Price, W. D.; Williams, E. R. *J. Phys. Chem. A* **1999**, *103*, 9266.

(19) Rak, J.; Skurski, P.; Simons, J.; Gutowski, M. *J. Am. Chem. Soc.* **2001**, *123*, 11695.

(20) Csonka, I. P.; Paizs, B.; Suhai, S. *J. Mass Spectrom.* **2004**, *39*, 1025.

(21) Gdanitz, R. J.; Cardoen, W.; Windus, T. L.; Simons, J. *J. Phys. Chem. A* **2004**, *108*, 515.

(22) Wyttenbach, T.; von Helden, G.; Bowers, M. T. *J. Am. Chem. Soc.* **1996**, *118*, 8355.

(23) Wyttenbach, T.; Bushnell, J. E.; Bowers, M. T. *J. Am. Chem. Soc.* **1998**, *120*, 5098.

(24) Wyttenbach, T.; Bowers, M. T. Gas-phase conformations: The ion mobility/ion chromatography method. In *Modern Mass Spectrometry*; Schalley, C. A., Ed.; Topics in Current Chemistry 225; Springer-Verlag: Berlin, 2003; pp 207−232.

(25) Wyttenbach, T.; Bowers, M. T. *J. Am. Soc. Mass Spectrom.* **1999**, *10*, 9.

(26) Cerda, B. A.; Cornett, L.; Wesdemiotis, C. *Int. J. Mass Spectrom.* **1999**, *193*, 205.

(27) Cerda, B. A.; Wesdemiotis, C. *Analyst* **2000**, *125*, 657.

(28) Rogalewicz, F.; Hoppilliard, Y.; Ohanessian, G. *Int. J. Mass Spectrom.* **2000**, *196*, 565.

(29) Farrugia, J. M.; O'Hair, R. A. J. *Int. J. Mass Spectrom.* **2003**, *222*, 229.

(30) Shek, P. Y. I.; Zhao, J.; Ke, Y.; Siu, K. W. M.; Hopkinson, A. C. *J. Phys. Chem. A* **2006**, *110*, 8282.

(31) Price, W. D.; Jockusch, R. A.; Williams, E. R. *J. Am. Chem. Soc.* **1997**, *119*, 11988.

(32) Schäfer, M.; Schmuck, C.; Geiger, L.; Chalmers, M. J.; Hendrickson, C. L.; Marshall, A. G. *Int. J. Mass Spectrom.* **2004**, *237*, 33.

(33) Kapota, C.; Lemaire, J.; Maître, P.; Ohanessian, G. *J. Am. Chem. Soc.* **2004**, *126*, 1836.

(34) Oomens, J.; Polfer, N.; Moore, D. T.; van der Meer, L.; Marshall, A. G.; Eyler, J. R.; Meijer, G.; von Helden, G. *Phys. Chem. Chem. Phys.* **2005**, *7*, 1345.

(35) Polfer, N. C.; Paizs, B.; Snoek, L. C.; Compagnon, I.; Suhai, S.; Meijer, G.; von Helden, G.; Oomens, J. *J. Am. Chem. Soc.* **2005**, *127*, 8571.

(36) Valle, J. J.; Eyler, J. R.; Oomens, J.; Moore, D. T.; van der Meer, A. F. G.; von Helden, G.; Meijer, G.; Hendrickson, C. L.; Marshall, A. G.; Blakney, G. T. *Rev. Sci. Instrum.* **2005**, *76*, 23103.

(37) Moore, D. T.; Oomens, J.; Eyler, J. R.; von Helden, G.; Meijer, G.; Dunbar, R. C. *J. Am. Chem. Soc.* **2005**, *127*, 7243.

(38) Dunbar, R. C.; Moore, D. T.; Oomens, J. *J. Phys. Chem. A* **2006**, *110*, 8316.

(39) Groenewold, G. S.; Gianotto, A. K.; Cossel, K. C.; Van Stipdonk, M. J.; Moore, D. T.; Polfer, N.; Oomens, J.; de Jong, W. A.; Visscher, L. *J. Am. Chem. Soc.* **2006**, *128*, 4802.

(40) Oomens, J.; Meijer, G.; von Helden, G. *Int. J. Mass Spectrom.* **2006**, *249*, 199.

(41) Oomens, J.; Sartakov, B. G.; Meijer, G.; von Helden, G. *Int. J. Mass Spectrom.* **2006**, *254*, 1.

(42) Polfer, N. C.; Oomens, J.; Dunbar, R. C. *Phys. Chem. Chem. Phys.* **2006**, *8*, 2744.
(43) Polfer, N. C.; Oomens, J.; Moore, D. T.; von Helden, G.; Meijer, G.; Dunbar, R. C. *J. Am. Chem. Soc.* **2006**, *128*, 517.
(44) Mac Aleese, L.; Simon, A.; McMahon, T. B.; Ortega, J. M.; Scuderi, D.; Lemaire, J.; Maître, P. *Int. J. Mass Spectrom.* **2006**, *249*, 14.
(45) Fridgen, T. D.; McMahon, T. B.; Maître, P.; Lemaire, J. *Phys. Chem. Chem. Phys.* **2006**, *8*, 2483.
(46) Fridgen, T. D.; MacAleese, L.; McMahon, T. B.; Lemaire, J.; Maître, P. *Phys. Chem. Chem. Phys.* **2006**, *8*, 955.
(47) Schäfer, M.; Polfer, N. C.; Oomens, J.; Blunk, D.; Forbes, M.; Jockusch, R. A. In *Proceedings of the 54th ASMS Conference on Mass Spectrometry and Allied Topics*, Seattle, WA, 2006.
(48) Kamariotis, A.; Boyarkin, O. V.; Mercier, S. R.; Beck, R. D.; Bush, M. F.; Williams, E. R.; Rizzo, T. R. *J. Am. Chem. Soc.* **2006**, *128*, 905.
(49) Oh, H. B.; Lin, C.; Hwang, H. Y.; Zhai, H. L.; Breuker, K.; Zabrouskov, V.; Carpenter, B. K.; McLafferty, F. W. *J. Am. Chem. Soc.* **2005**, *127*, 4076.
(50) Oh, H.; Breuker, K.; Sze, S. K.; Ge, Y.; Carpenter, B. K.; McLafferty, F. W. *Proc. Natl. Acad. Sci. U.S.A.* **2002**, *99*, 15863.
(51) Bush, M. F.; O'Brien, J. T.; Prell, J. S.; Saykally, R. J.; Williams, E. R. *J. Am. Chem. Soc.* **2007**, *129*, 1612.
(52) Simon, A.; MacAleese, L.; Maître, P.; Lemaire, J.; McMahon, T. B. *J. Am. Chem. Soc.* **2007**, *129*, 2829.
(53) Oomens, J.; Tielens, A.; Sartakov, B. G.; von Helden, G.; Meijer, G. *Astrophys. J.* **2003**, *591*, 968.
(54) Wu, R. H.; McMahon, T. B. *Angew. Chem., Int. Ed.* **2007**, *46*, 3668.
(55) Wu, R. H.; McMahon, T. B. *J. Am. Chem. Soc.* **2007**, *129*, 4864.
(56) Geller, O.; Lifshitz, C. *J. Phys. Chem. A* **2003**, *107*, 5654.
(57) Cox, H. A.; Julian, R. R.; Lee, S. W.; Beauchamp, J. L. *J. Am. Chem. Soc.* **2004**, *126*, 6485.
(58) Rožman, M.; Srzic, D.; Klasinc, L. *Int. J. Mass Spectrom.* **2006**, *253*, 201.
(59) Chapo, C. J.; Paul, J. B.; Provencal, R. A.; Roth, K.; Saykally, R. J. *J. Am. Chem. Soc.* **1998**, *120*, 12956.
(60) Oepts, D.; van der Meer, A. F. G.; van Amersfoort, P. W. *Infrared Phys. Technol.* **1995**, *36*, 297.
(61) Prazeres, R.; Glotin, F.; Insa, C.; Jaroszynski, D. A.; Ortega, J. M. *Eur. Phys. J. D* **1998**, *3*, 87.
(62) Wilson, R. G.; Brewar, G. R. *Ion Beams; With Applications to Ion Implantation*; Wiley: New York, 1973; p 266.
(63) Meyer, F.; Chen, Y. M.; Armentrout, P. B. *J. Am. Chem. Soc.* **1995**, *117*, 4071.
(64) Walter, D.; Sievers, M. R.; Armentrout, P. B. *Int. J. Mass Spectrom.* **1998**, *175*, 93.
(65) Rodgers, M. T.; Armentrout, P. B. *Mass Spectrom. Rev.* **2000**, *19*, 215.
(66) El Aribi, H.; Rodriquez, C. F.; Shoeib, T.; Ling, Y.; Hopkinson, A. C.; Siu, K. W. M. *J. Phys. Chem. A* **2002**, *106*, 8798.
(67) Senko, M. W.; Canterbury, J. D.; Guan, S. H.; Marshall, A. G. *Rapid Commun. Mass Spectrom.* **1996**, *10*, 1839.
(68) Halgren, T. A. *J. Am. Chem. Soc.* **1992**, *114*, 7827.
(69) Leininger, T.; Nicklass, A.; Kuchle, W.; Stoll, H.; Dolg, M.; Bergner, A. *Chem. Phys. Lett.* **1996**, *255*, 274.
(70) Frisch, M. J.; Trucks, G. W.; Schlegel, H. B.; Scuseria, G. E.; Robb, M. A.; Cheeseman, J. R.; Montgomery, J. A., Jr.; Vreven, T.; Kudin, K. N.; Burant, J. C.; Millam, J. M.; Iyengar, S. S.; Tomasi, J.; Barone, V.; Mennucci, B.; Cossi, M.; Scalmani, G.; Rega, N.; Petersson, G. A.; Nakatsuji, H.; Hada, M.; Ehara, M.; Toyota, K.; Fukuda, R.; Hasegawa, J.; Ishida, M.; Nakajima, T.; Honda, Y.; Kitao, O.; Nakai, H.; Klene, M.; Li, X.; Knox, J. E.; Hratchian, H. P.; Cross, J. B.; Bakken, V.; Adamo, C.; Jaramillo, J.; Gomperts, R.; Stratmann, R. E.; Yazyev, O.; Austin, A. J.; Cammi, R.; Pomelli, C.; Ochterski, J. W.; Ayala, P. Y.; Morokuma, K.; Voth, G. A.; Salvador, P.; Dannenberg, J. J.; Zakrzewski, V. G.; Dapprich, S.; Daniels, A. D.; Strain, M. C.; Farkas, O.; Malick, D. K.; Rabuck, A. D.; Raghavachari, K.; Foresman, J. B.; Ortiz, J. V.; Cui, Q.; Baboul, A. G.; Clifford, S.; Cioslowski, J.; Stefanov, B. B.; Liu, G.; Liashenko, A.; Piskorz, P.; Komaromi, I.; Martin, R. L.; Fox, D. J.; Keith, T.; Al-Laham, M. A.; Peng, C. Y.; Nanayakkara, A.; Challacombe, M.; Gill, P. M. W.; Johnson, B.; Chen, W.; Wong, M. W.; Gonzalez, C.; Pople, J. A. *Gaussian 03*, revision D.01; Gaussian, Inc.: Wallingford, CT, 2004.
(71) Shoeib, T.; Siu, K. W. M.; Hopkinson, A. C. *J. Phys. Chem. A* **2002**, *106*, 6121.
(72) El Aribi, H.; Shoeib, T.; Ling, Y.; Rodriquez, C. F.; Hopkinson, A. C.; Siu, K. W. M. *J. Phys. Chem. A* **2002**, *106*, 2908.
(73) Cotton, F.; Wilkinson, G.; Murillo, C.; Bochmann, M. *Advanced Inorganic Chemistry*, 6th ed.; John Wiley & Sons: Toronto, 1999; p 1089.